Incident angle dependence of Pi-SAR polarimetric scattering characteristics

Koichi IRIBE†, Motoyuki SATO‡
†Graduate school of Environmental studies, Tohoku University
iribe@cneas.tohoku.ac.jp
‡Center for Northeast Asian Studies, Tohoku University
Kawauchi, Sendai, 980-8576, Japan
sato@cneas.tohoku.ac.jp

1. Introduction

Polarimetric and interferometric synthetic aperture radars (SAR) have widely been used for observing the Earth's surface. One of such systems is the Pi-SAR (Polarimetric and Interferometric SAR) system, jointly developed by the CRL and JAXA (formerly NASDA). Pi-SAR is an airborne high resolution imaging radar system which has fully polarimetric X-band SAR and L-band SAR and the X-band has two receiving antennas located in cross-track direction for interferometric observation and can image the Earth's surface at any time of day or night under any atmospheric conditions. Because of its multi-parameter measurement capability, this radar system can be considered as one of the most powerful tools for investigation of the Earth's surface [1].

It is well known that the polarimetric scattering characteristic of microwave is dependent on the incident angle [2]. In this study, we analyze the polarimetric scattering characteristics of Pi-SAR data of Sendai city in relation to the incident angle. While we observed the polarimetric characteristics of different features in urban areas, the co-polarized scattering was dominant, however, at certain buildings in a certain area cross-polarized scattering became dominant. This means that the polarimetric scattering changes in relation to the incident angles as well as the orientation of the buildings.

In order to explain the variation of polarimetric scattering in the urban area, we introduced a simple double bounce model. For this aim, initially we apply polarimetric entropy analysis to the selected Pi-SAR data to extract pixels in which double bounce effects are observed. Then, we plot the polarimetric scattering characteristics of pixels in relation to the incident angles and conduct the related analysis.

2. The Double bounce model of a microwave

The schematic view of the model of a double bounce scattering is shown in Figure 1. Here, θ_i is the incident angle of microwave, ε and μ are the permittivity and the permeability of each medium, respectively. The double bounce wave is received by the Pi-SAR monostatic radar as a backscattering wave. Due to a incident plane of a microwave, we can consider that the transverse electric (TE) polarization corresponds to HH polarization and the transverse magnetic (TM) polarization corresponds to VV polarization and the scattering characteristics of HH and VV polarization form the reflection coefficients of TE and TM wave in relation to the incident angles. The reflection coefficient of a double bounce wave can be estimated by multiplying the Fresnel reflection coefficient of the boundary between Medium 1 and Medium 2 and that of the boundary between Medium 1 and Medium 3. The two curves shown in Figure 2 show the reflection coefficients of HH and VV polarization as a

ISBN: 4-88552-207-2 C3055©IEICE

function of the incident angle. For the estimation, we used $\varepsilon_1 = 1, \varepsilon_2 = \varepsilon_3 = 7$, and $\mu_1 = \mu_2 = \mu_3 = 1$.

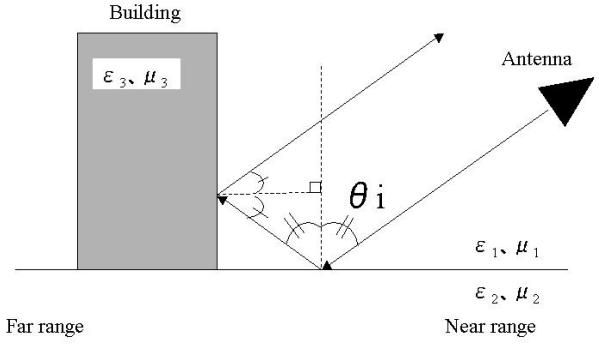

Figure 1. The schematic view of the double bounce model

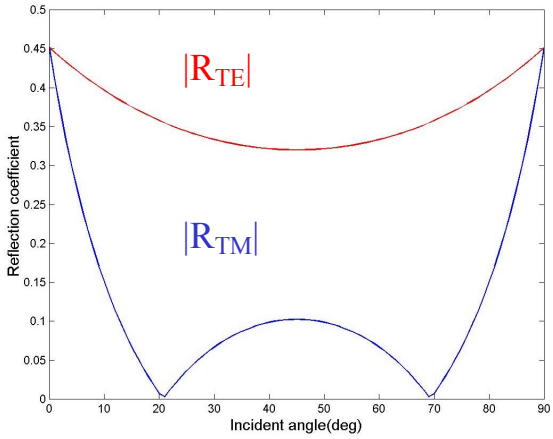

Figure 2. The reflection coefficients $\varepsilon_1 = 1, \varepsilon_2 = \varepsilon_3 = 7$ and $\mu_1 = \mu_2 = \mu_3 = 1$

3. Polarimetric entropy analysis for Pi-SAR data

In order to compare Pi-SAR data with the double bounce model, we have to select the targets in which the double bounce effect was taken place. However, from the primary Pi-SAR image it is difficult to observe whether a double bounce effect has taken place or not at the observed targets. Therefore, for discrimination among the scattering mechanisms observed at the selected targets, a polarimetric entropy analysis was used [3]. This analysis defines the entropy (H) and the angle ($\bar{\alpha}$) and classifies the scattering characteristics of pixels by using a mechanism and a randomness of the polarimetric scattering. Using this method, one can extract the information about a double bounce scattering as well as other scattering properties of different targets.

Initially, we calculated H and $\bar{\alpha}$ by pixels and then, plotted them to a H-$\bar{\alpha}$ color plane shown in Figure 3. After that we evaluated the scattering characteristics of targets from their position and then, plotted a color of the H-$\bar{\alpha}$ plane to each pixel.

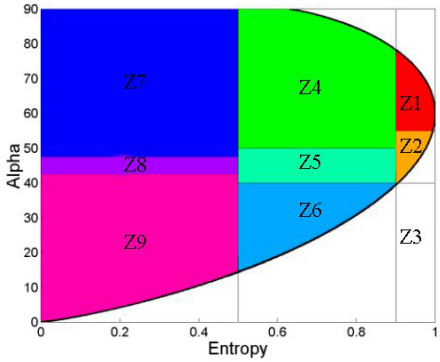

Figure3. H-$\bar{\alpha}$ plane

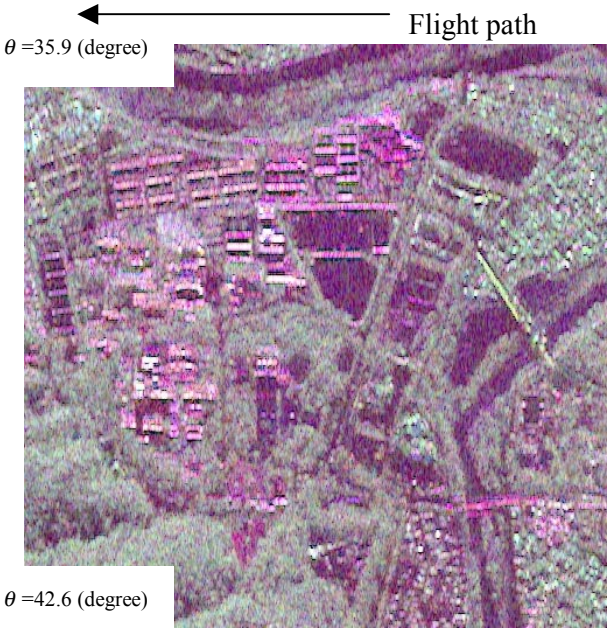

Figure 4. Fully polarimetric Pi-SAR image
L-band, June. 12, 2002, Cloudy ©NASDA
1250m*1250m (R: HH, G: HV, B: VV)
Tohoku University, Kawauchi campus

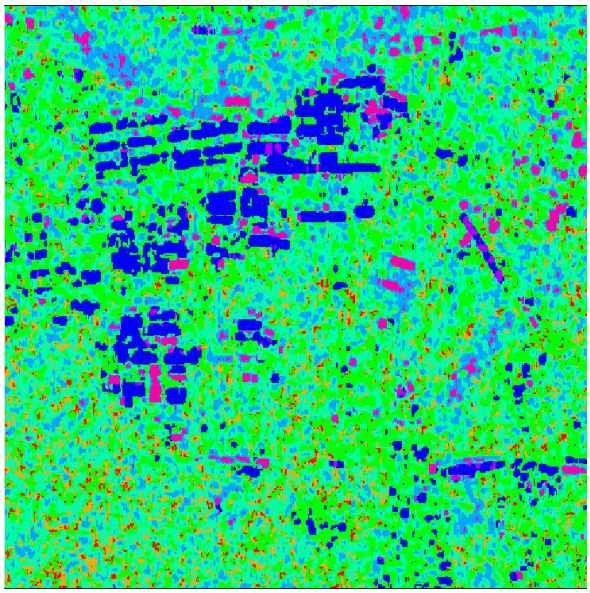

Figure 5. H-$\bar{\alpha}$ color plotted image
L-band, June. 12, 2002, 1250m*1250m
Tohoku University, Kawauchi campus

Figure 4 shows the polarimetric Pi-SAR L-band image of Tohoku University Kawauchi campus area, and Figure 5 shows the result of the polarimetric entropy analysis for the same area. In Figure 5, the blue color (Z7) represents a single scattering property of a diplane. Therefore, we can consider that in these targets, which are mostly buildings a double bounce effect was taking place.

4. A comparison between the observation data and the model

In order to compare the polarimetric scattering characteristics of the observation data with the double bounce model, we used Pi-SAR data of Sendai taken at two different flight paths shown in Figure 7.

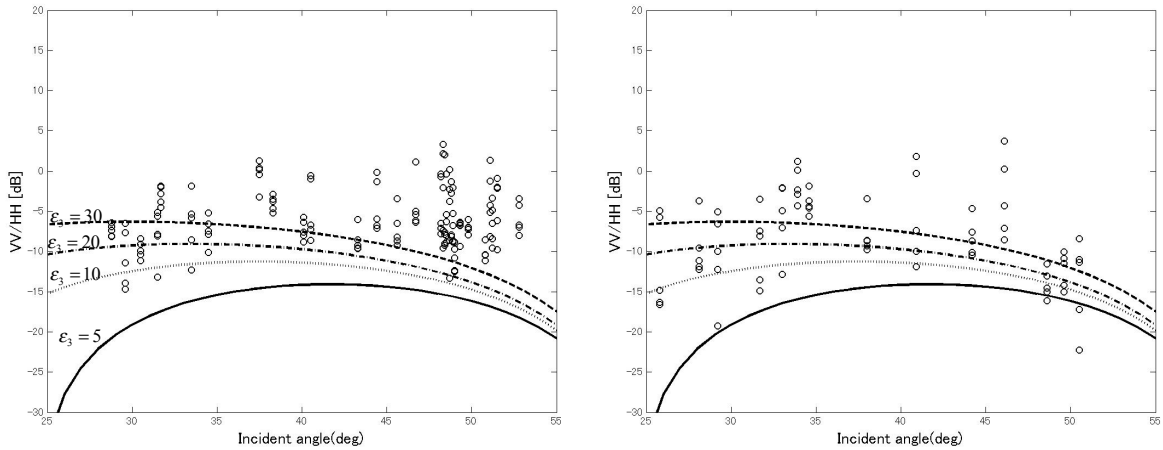

Sendai5911 Sendai5910

Figure 6. The polarimetric scattering characteristics to the incident angle
Small circle: Pi-SAR data. Continuous line: $\varepsilon_1 = 1, \varepsilon_2 = 3, \varepsilon_3 = 5$. Dashed line: $\varepsilon_1 = 1, \varepsilon_2 = 3, \varepsilon_3 = 10$.
Chained line: $\varepsilon_1 = 1, \varepsilon_2 = 3, \varepsilon_3 = 20$. Dotted line: $\varepsilon_1 = 1, \varepsilon_2 = 3, \varepsilon_3 = 30$.

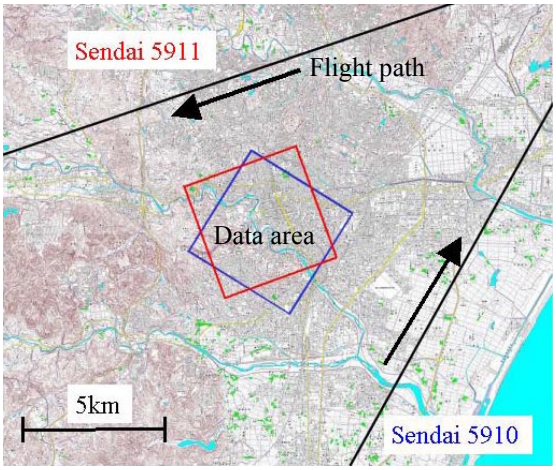

Figure 7. The flight paths over Sendai

We acquired the ratio of VV and HH polarization for each pixel which represent a double bounce, and plotted it to the incident angle. By taking the ratio of S_{VV} to S_{HH}, we can cancel the effects of the attenuation due to the propagation path and the imbalance occurred between the antennas. Figures 6 shows the results of the analysis. In the figure, a continuous line shows the condition of $\varepsilon_1 = 1, \varepsilon_2 = 3, \varepsilon_3 = 5$, a dashed line shows the condition of $\varepsilon_1 = 1, \varepsilon_2 = 3, \varepsilon_3 = 10$, a chained line shows the condition of $\varepsilon_1 = 1, \varepsilon_2 = 3, \varepsilon_3 = 20$, and a dotted line shows the condition of $\varepsilon_1 = 1, \varepsilon_2 = 3, \varepsilon_3 = 30$. The relative pemittivity of the asphalt is 2.7, while for the glass it is in between 5.4 and 9.9. Black circles show the polarimetric scattering characteristics of the targets in relation to the incident angles of a microwave. As seen from the figures, the theoretical curves of the polarimetric scattering characteristics vary by the permittivity of the medium and the polarimetric scattering characteristics of the targets are different to some extent in spite of the same incident angle. However, the data used in this study represent a part of the overall data and fall into narrow incident angles. To conduct more refined analysis, we need to have the data can cover a large range of the incident angles.

5. Conclusion

The aim of this study was to conduct polarimetric scattering analysis in relation to the incident angles comparing the proposed double bounce model with Pi-SAR data. In order to select the targets from Pi-SAR image, we carried out the polarimetric entropy analysis and detected the objects where double bounce effects took place. However, from this study we could not make a final conclusion because the width of the incident angles of the selected image that we analyzed was not broad enough. Nevertheless, one could at least see some tendencies of the polarimetric scattering characteristics in relation to the incident angles. In the next step we will conduct the same analysis for the images having more broad incident angles. Furthermore, the influence of the orientation angle of targets will be analyzed.

6. Acknowledgements

In this paper, we used Pi-SAR data observed on June 12th 2002. We thank to CRL and JAXA for providing Pi-SAR data.

7. References

[1] Sato, M., Koike, T., “Classification of Tree Type by Polarimetric Pi-SAR,” Proc. IEEE Int. Symp Geoscience and Remote Sensing, IGARASS2003, Toulouse, France, July 2003.

[2] Cloude, S.R. and Papathanassiou, K.P., “Polarimetric SAR interferometry,” IEEE Trans. Geosci. Remote Sensing, vol. 36, no. 5, pp.1551-1565, Sept. 1998.

[3] Cloude, S.R. and Pottier, E., “An Entropy Based Classification Scheme for Land Applications of Polarimetric SAR,” IEEE Trans. Geosci. Remote Sensing, vol. 35, no. 1, pp.68-78, Jan. 1997.